Synchronization and amplitude death in hypernetworks

Shakir Bilal[1] and Ramakrishna Ramaswamy[1,2]
[1]*School of Physical Sciences, Jawaharlal Nehru University, New Delhi 110 067, India*
[2]*University of Hyderabad, Hyderabad 500 046, India*
(Received 31 December 2013; revised manuscript received 23 March 2014; published 27 June 2014)

We study dynamical systems on a *hypernetwork*, namely by coupling them through several variables. For the case when the coupling(s) are all linear, a comprehensive analysis of the master stability function (MSF) for synchronized dynamics is presented and, through application to a number of paradigmatic examples, the typical forms of the MSF are discussed. The MSF formalism for hypernetworks also provides a framework to study synchronization in systems that are diffusively coupled through dissimilar variables—the so-called conjugate coupling that can lead to amplitude or oscillation death.

DOI: 10.1103/PhysRevE.89.062923 PACS number(s): 05.45.Xt

I. INTRODUCTION

The dynamics of specific isolated systems, and the manner in which these are modified when coupled to other similar or dissimilar systems, have been systematically studied [1–4] in numerous settings. The unexpected dynamical states that can result when nonlinear dynamical systems are coupled have been widely explored in a variety of contexts that include physical, chemical, biological, ecological, and even social systems [4–9].

The nature of the coupling between systems is significant. When the coupling is linear and weak, some of the behavior of the coupled system can be deduced from the uncoupled case through a perturbative analysis. Other cases are less amenable to analysis, but these also occur quite naturally, as for instance nonlinear coupling [10] or coupling via dissimilar variables, namely conjugate coupling [2,3,11,12].

Our interest here is in multiply coupled dynamical systems, namely the case of *hypernetworks* [13]. This situation is frequently encountered in experimental situations that involve spatially extended dynamical systems [14] and the case of linear coupling through a single variable is often an inadequate approximation [15]. This is therefore a natural setting within which to treat coupled systems, and, as we discuss below, the case of coupling via dissimilar variables [2] can also be viewed as a hypernetwork [13].

We consider the simplest cases, when the couplings are all taken to be linear in the variables. Two effects that we study are the occurrence of amplitude death (AD) [16–19] and synchronization [4] in hypernetworks. There is a well-developed formalism that applies in the analysis of the many forms of synchronization that are observed in nonlinear dynamical systems [4,20,21]. Synchronized dynamics occurs in a subspace of the overall phase space, the synchronization manifold [22], and the principal condition for the occurrence of such dynamics relates to the stability of this manifold. This can be studied via the master stability function (MSF) [21,23–25].

The MSF provides a complete classification and a detailed understanding of the stability conditions for various forms of synchrony in simple networks [26]. We extend this analysis and study the MSF formalism for hypernetworks to determine whether these can also be classified into distinct sets. A combination of numerical as well as analytical methods is used to analyze well-studied flows such as the chaotic Rössler, Lorenz, and driven van der Pol and Duffing oscillators, as well as excitable systems such as the Hindmarsh-Rose neuronal model.

The phenomenon of synchronization in systems coupled through dissimilar variables is well described within the hypernetwork MSF formalism, subsequently providing a general understanding of conjugate diffusive coupling. The MSFs observed here typically fall into three basic classes. In the first class, there is no regime of synchronization. The other two types correspond to bounded or unbounded regions of synchronization.

The overall organization of this paper is as follows. We start in Sec. II by introducing the notation and the notion of hypernetworks, and briefly review the MSF formalism that applies. In Sec. III numerical results are presented for the MSF using the model flows mentioned above, and a case for classifying the MSFs into distinct types is made. The paper concludes with a discussion and summary in Sec. IV.

II. HYPERNETWORK COUPLING

Consider a dynamical system in n dimensions,

$$\dot{\mathbf{x}} = \mathbf{F}(\mathbf{x},\boldsymbol{\mu}), \tag{1}$$

where $\mathbf{x} \equiv \{x_1, x_2, \ldots, x_n\}$ and $\boldsymbol{\mu}$ denotes the parameters that govern the flow. When two or more such systems are coupled linearly with each other via more than one variable, very generally we can write the set of coupled equations as

$$\dot{\mathbf{x}}^i = \mathbf{F}(\mathbf{x}^i,\boldsymbol{\mu}^i) + \sum_k \varepsilon^k \sum_j^N G_{ij}^k \mathbf{H}^k(\mathbf{x}^j). \tag{2}$$

The superscript i that takes the value from $1,\ldots,N$ refers to the individual systems. $\mathbf{G}^k$ and $\mathbf{H}^k$ are matrices that specify the coupling of the underlying hypernetwork, and their matrix elements are denoted G_{ij}^k and H_{ij}^k, respectively. The coupling strength corresponding to each of the coupled variables is ε^k, and in this paper we consider only two distinct variables for coupling; therefore, k takes values 1,2. Denoting by $\mathbf{X}$ the complete set of nN variables (n being the dimension of the systems at each node and N being the total number of nodes in the underlying network) the above equations of motion can

be written compactly as

$$\dot{\mathbf{X}} = \mathbf{I} \otimes \mathbf{F}(\mathbf{x},\boldsymbol{\mu}) + \varepsilon^1 \mathbf{G}^1 \otimes \mathbf{H}^1 + \varepsilon^2 \mathbf{G}^2 \otimes \mathbf{H}^2, \tag{3}$$

where $\mathbf{I}$ is the $N \times N$ identity matrix, while the matrices $\mathbf{G}^k$ are $N \times N$ since there are N nodes in the underlying network and the matrices $\mathbf{H}^k$, $k = 1,2$, are $n \times n$ since each individual node corresponds to an n-dimensional flow. In all the examples we study here, the matrices $\mathbf{G}^k$ commute and their row sums are constants, $\sum_j G^k_{ij} = \delta^k, k = 1,2$. When the systems on the individual nodes are synchronized, then the synchronization state ($\mathbf{x}^1 = \mathbf{x}^2 = \cdots = \mathbf{x}^N \equiv \mathbf{x}^{\mathrm{S}}$) dynamics is given by

$$\dot{\mathbf{x}}^{\mathrm{S}} = \mathbf{F}(\mathbf{x}^{\mathrm{S}},\boldsymbol{\mu}) + \varepsilon^1 \delta^1 \mathbf{H}^1(\mathbf{x}^{\mathrm{S}}) + \varepsilon^2 \delta^2 \mathbf{H}^2(\mathbf{x}^{\mathrm{S}}). \tag{4}$$

It is useful to consider, as a specific example, identical coupled Rössler oscillators, each of which is specified by the evolution equations (A1) with the two systems coupled bidirectionally in two variables on the hypernetwork,

$$\begin{aligned} \dot{x}^i_1 &= -a x^i_2 - x^i_3 + \varepsilon^1\big((1-\nu)x^j_1 - x^i_1\big) \\ &\quad + \varepsilon^2\big(x^j_2 - (1-\nu)x^i_2\big), \\ \dot{x}^i_2 &= a x^i_1 + b x^i_2, \quad \dot{x}^i_3 = c + x^i_3\big(x^i_1 - d\big). \end{aligned} \tag{5}$$

The additional parameter ν can be used to further tune the nature of the coupling. With reference to Eq. (3), the matrices specifying the coupling in Eq. (5) are

$$\mathbf{G}^1(\nu) = \begin{pmatrix} -1 & 1-\nu \\ 1-\nu & -1 \end{pmatrix}, \quad \mathbf{H}^1 = \begin{pmatrix} 1 & 0 & 0 \\ 0 & 0 & 0 \\ 0 & 0 & 0 \end{pmatrix},$$

$$\mathbf{G}^2(\nu) = \begin{pmatrix} -(1-\nu) & 1 \\ 1 & -(1-\nu) \end{pmatrix}, \quad \mathbf{H}^2 = \begin{pmatrix} 0 & 1 & 0 \\ 0 & 0 & 0 \\ 0 & 0 & 0 \end{pmatrix}. \tag{6}$$

Following the convention [21,26] used in writing the matrices in Eq. (6) from Eq. (5), the nonzero elements in the matrices $\mathbf{H}^k$ are indicated by the notation $i \to j$ to signify that the ith component of one node is coupled to the jth component of another. On the hypernetwork, there can be multiple connections in either direction. There is some arbitrariness in which of the coupling terms is assigned to $\mathbf{H}^1$ and $\mathbf{H}^2$, and we choose an internally consistent convention [27].

The stability of the synchronization manifold Eq. (4) is governed by the variational equation associated with Eq. (3). We obtain the variational equation for systems with identical and nonidentical parameters, respectively, below.

A. Identical parameters

By considering variations evaluated on the synchronization manifold it is straightforward to obtain from Eq. (3),

$$\begin{aligned} \dot{\boldsymbol{\xi}} &= \mathbf{I} \otimes \mathbf{DF}(\mathbf{x}^{\mathrm{S}},\boldsymbol{\mu})\boldsymbol{\xi} + \varepsilon^1 \mathbf{G}^1 \otimes \mathbf{DH}^1(\mathbf{x}^{\mathrm{S}})\boldsymbol{\xi} \\ &\quad + \varepsilon^2 \mathbf{G}^2 \otimes \mathbf{DH}^2(\mathbf{x}^{\mathrm{S}})\boldsymbol{\xi}, \end{aligned} \tag{7}$$

where $\boldsymbol{\xi} = \{\boldsymbol{\xi}^1, \ldots, \boldsymbol{\xi}^N\}$ is a nN-dimensional vector, $\boldsymbol{\xi}^i$ are n-dimensional vectors, and $\mathbf{x}^{\mathrm{S}}$ is obtained by integrating Eq. (4). The matrix $\mathbf{I} \otimes \mathbf{DF}(\mathbf{x}^{\mathrm{S}},\boldsymbol{\mu})$ is block diagonal. If the matrices $\mathbf{G}^k$ are simultaneously diagonalizable by the same orthogonal transformation $\mathbf{P}$, i.e., $\mathbf{G}^k = \mathbf{P}^{-1}\boldsymbol{\Lambda}^k\mathbf{P}$ for both $k = 1,2$, then Eq. (7) reduces to a block diagonal form. The dynamics of the qth block, where q takes integer values from $1, \ldots, N$, is given by

$$\dot{\boldsymbol{\xi}}_q = \mathbf{DF}(\mathbf{x}^{\mathrm{S}},\boldsymbol{\mu})\boldsymbol{\xi}_q + g^1_q \mathbf{DH}^1(\mathbf{x})\boldsymbol{\xi}_q + g^2_q \mathbf{DH}^2(\mathbf{x})\boldsymbol{\xi}_q, \tag{8}$$

where $\boldsymbol{\xi}_q$ are n-dimensional vectors, and g^k_q are the eigenvalues of $\mathbf{G}^k$, which may be complex in general. Since the equation for each block is identical, Eq. (8) can be written as

$$\begin{aligned} \dot{\boldsymbol{\zeta}} &= \mathbf{DF}(\mathbf{x}^{\mathrm{S}},\boldsymbol{\mu})\boldsymbol{\zeta} + (\alpha^1 + i\beta^1)\mathbf{DH}^1(\mathbf{x}^{\mathrm{S}})\boldsymbol{\zeta} \\ &\quad + (\alpha^2 + i\beta^2)\mathbf{DH}^2(\mathbf{x}^{\mathrm{S}})\boldsymbol{\zeta}, \end{aligned} \tag{9}$$

where $\boldsymbol{\zeta}$ is an n-dimensional vector, and α^k and β^k are the real and imaginary parts of the rescaled eigenvalues of $\mathbf{G}^k$. As has been discussed earlier [21,26], by varying these one can recover the dynamics for each of the q modes of the variational equations (8). If the Lyapunov exponent transverse to the synchronization manifold λ_s, namely the master stability function [21], is less than zero, the synchronization is stable. For the symmetric matrices $\mathbf{G}^k$ in Eq. (3) the imaginary part of the eigenvalues $\beta^k = 0$, $k = 1,2$.

B. Parameter and coupling strength mismatch

In case of parameter mismatch the variational equation becomes, following [28–30],

$$\begin{aligned} \dot{\boldsymbol{\zeta}} &= \mathbf{DF}(\bar{\mathbf{x}},\bar{\boldsymbol{\mu}})\boldsymbol{\zeta} + \alpha^1 \mathbf{DH}^1\boldsymbol{\zeta} + \alpha^2 \mathbf{DH}^2\boldsymbol{\zeta} \\ &\quad + \psi^1 \mathbf{D}_{\boldsymbol{\mu}}\mathbf{F}(\bar{\mathbf{x}},\bar{\boldsymbol{\mu}}) + \psi^2 \mathbf{D}_{\boldsymbol{\mu}}\mathbf{DF}(\bar{\mathbf{x}},\bar{\boldsymbol{\mu}})\boldsymbol{\zeta}. \end{aligned} \tag{10}$$

Here bar over a variable or parameter implies population average. When the perturbations due to $\{\psi^k\}$ are small the average $\bar{\mathbf{x}}$ can be replaced with the synchronization manifold $\mathbf{x}^{\mathrm{S}}$ as obtained from integrating Eq. (4) at the average value of parameters $\bar{\boldsymbol{\mu}}$. Here ψ^1 and ψ^2 represent the strength of first- and second-order terms in the Taylor expansion [28–30] that are linear in parameter mismatch. For mismatch in the parameter a for the Rössler flow Eq. (A1), we have $\mathbf{D}_{\boldsymbol{\mu}}\mathbf{F} = [-x_2, x_1, 1]^T$ and $\mathbf{D}_{\boldsymbol{\mu}}\mathbf{DF} = [[0,-1,0],[1,0,1],[0,0,0]]$.

The unequal coupling strengths can be achieved in two ways within the MSF formalism. Choose (a) matrices $\mathbf{G}^1$ and $\mathbf{G}^2$ such that the absolute value of row sums are related to each other by a scale factor, or (b) different values of ε^1 and ϵ^2. In both these cases the rescaled eigenvalues α^1 and α^2 will be related by a factor $\alpha^1 = \kappa\alpha^2$, but the synchronized solutions may or may not be those of the uncoupled case as determined by Eq. (4) with $\delta^k = 0$, $k = 1,2$.

C. Synchronization and amplitude death: Rössler flow

For coupled Rössler flows as in Eq. (5), when $\varepsilon^1 = \varepsilon^2$ and $\nu = 1$, the conjugate diffusive coupling [3] is recovered. This limit is known to produce the phenomenon of amplitude death [2]. Further the transition to synchronization in that limit is accompanied by chaos suppression [3,31]. Furthermore, the synchronized dynamics is not present in the uncoupled system.

Chaos suppression here corresponds to a transition from chaotic dynamics ($\lambda_1 > 0$) to a periodic orbit ($\lambda_1 = 0$) [3,31]. For the hypernetwork coupling above, note that $\nu = 1$ gives $|\delta^k| = \nu = 1$ (the row sum of G^k in Eq. (6)), and thus the synchronized dynamics given by Eq. (4) does not reduce

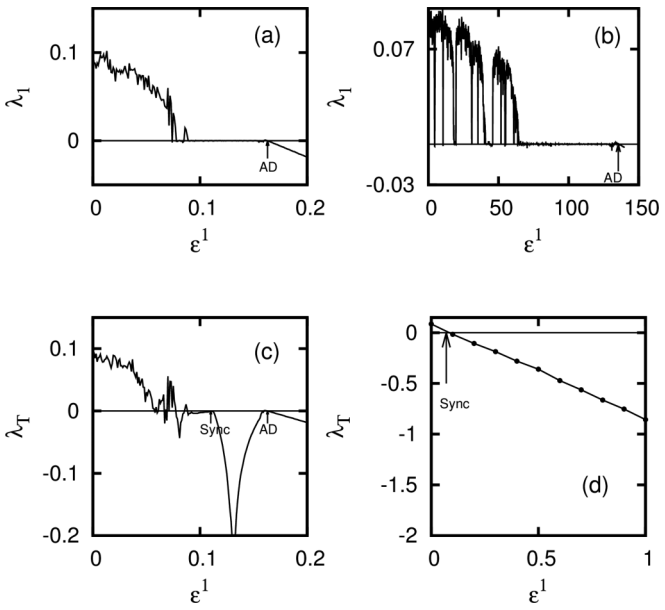

FIG. 1. Largest Lyapunov exponent, λ_1, and the transverse Lyapunov exponent λ_T for a hypernetwork of two nodes, each with a Rössler oscillator, as a function of the coupling strength ε^1 ($\varepsilon^2 = \varepsilon^1$). In (a) and (c) the parameter $\nu = 1$, while for (b) and (d), $\nu = 0.0012$. The point of synchronization is easily checked by computing the eigenvalues of the matrices $\mathbf{G}^k$ in Eq. (6).

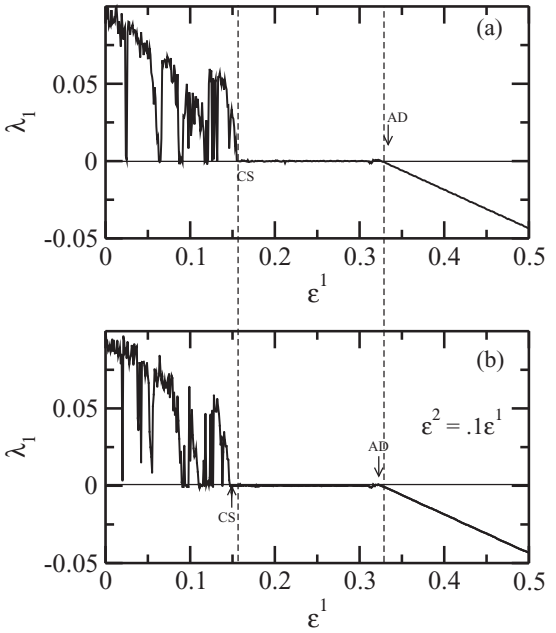

FIG. 2. Largest Lyapunov exponent for two coupled Rössler flows with the matrices $\mathbf{G}^k$, $\mathbf{H}^k$ given in Eq. (6), with $\nu = 0.5$. In (a) the eigenvalues of the two connection matrices are the same and in (b) the coupling strengths are $\varepsilon^2 = 0.1\varepsilon^1$ (namely the eigenvalues are rescaled as $\alpha^2 = 0.1\alpha^1$; see the text for explanation). The transition points to amplitude death and chaos suppression are marked AD and CS, respectively.

to the uncoupled flow. Clearly then for all $0 < \nu < 1$ the synchronized dynamics is actually *not* present in the uncoupled flow, but in such cases we find that amplitude death is still observed. Conjugate diffusive coupling [3] is thus a special case in the hypernetwork.

When $\nu = 0$ the row sums of each of the connectivity matrices $\delta^{1,2}$ is zero and hence the dynamics on the synchronization manifold is governed by the uncoupled equation. We find that amplitude death can be observed for a general conjugate diffusive coupling as in Eq. (5) even for $\nu \sim 0$ as shown in Fig. 1. However, this is absent for $\nu = 0$. It was noted in [3] that transition to synchronization coincides with chaos suppression, but a change in the parameter ν away from unity and towards zero shows that synchronization precedes chaos suppression (Fig. 1). It is already known that parameter mismatch in coupled dynamical systems can lead to amplitude death [32–34]. Shown in Fig. 2 is the largest Lyapunov exponent of the system in Eq. (2) and it is clear that amplitude death persists for the case of nonidentical coupling strengths, i.e., for ratio of coupling strengths different from unity, on the hypernetwork.

While the results presented are for Rössler oscillators, we have obtained similar results for two coupled Lorenz systems. In the following sections we will classify the MSFs as obtained from Eq. (9) using different flows and test their robustness under perturbations as in Eq. (10).

III. MSF FOR TYPICAL NONLINEAR FLOWS

The behavior of the MSF for hypernetworks can be classified into categories following Lai *et al.* [26]. When there is a single coupling matrix the MSF can be characterized by the number of times it crosses the zero axis [26] as a function of rescaled eigenvalue. Such an MSF is said to belong to the class $\Gamma^k_m, k = 1,2$, where m is the number of zero axis crossings.

Shown in Figs. 3 and 4 are the MSFs for the flows listed in the Appendix under the coupling schemes indicated in the figures. Broadly speaking, three classes of MSF are observed.

(i) No region of negative MSF, i.e., no synchronization possible.

(ii) Unbounded regions of negative MSF in the α^1-α^2 plane.

(iii) Bounded region(s) of negative (positive) MSF surrounded by positive (negative) MSF.

These categories arise out of the following generic behavior. If the MSF crosses the zero axis once when one of the parameters α^k is varied while the other $\alpha^l = 0$, where $[k,l] = 1,2$ but $k \neq l$, then a small nonzero value of α^l has one of the following effects: increasing or decreasing the interval of negative MSF in α^k. This change in the interval of negative MSF may or may not be monotonic. A combination of these possibilities helps create bounded or unbounded regions of stability as evident in Figs. 3 and 4. In Figs. 3 through 6, the contours of the MSF are plotted in the α^1-α^2 plane, with the contour in black representing the zero value of the MSF and other contours corresponding to the numerical values given in the respective figure captions. Note that the α^k are the real parts of the eigenvalues of the matrices $\mathbf{H}^k$ [27].

Thus the MSF in a hypernetwork can be classified into three categories: systems where there is no synchronization, when there are unbounded regions of synchronization, and when there are closed or bounded regions in parameter space, of stable and unstable synchronized dynamics. These typical

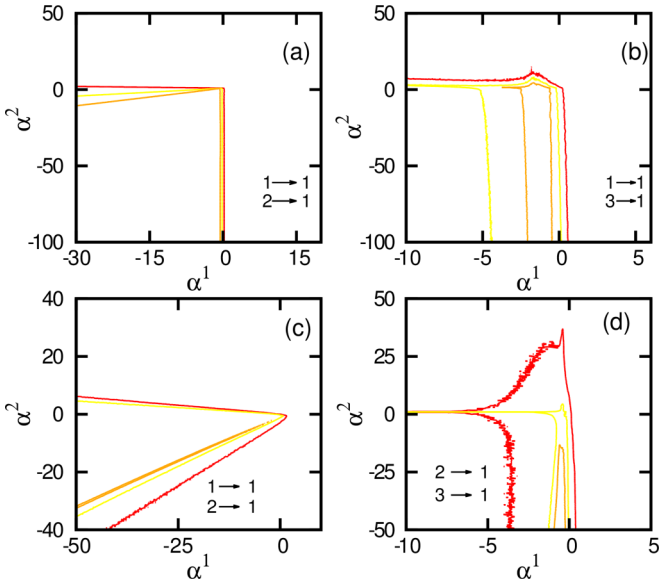

FIG. 3. (Color online) Contours of constant MSF (λ_s) with coupling schemes as indicated by the pair of arrows, on a hypernetwork. Figures (a) and (b) are for coupled Rössler flows, and the contours correspond to $\lambda_s = 0.2, 0.0, -0.2$. Figures (c) and (d) are for Hindmarsh-Rose neuronal systems. In (c) the contours correspond to $\lambda_s = -0.08, 0.0, 0.1$, while in (d) the contours correspond to $\lambda_s = -0.1, 0.0, 0.2$. The color code for the contours is positive (red), negative (orange), and zero (yellow).

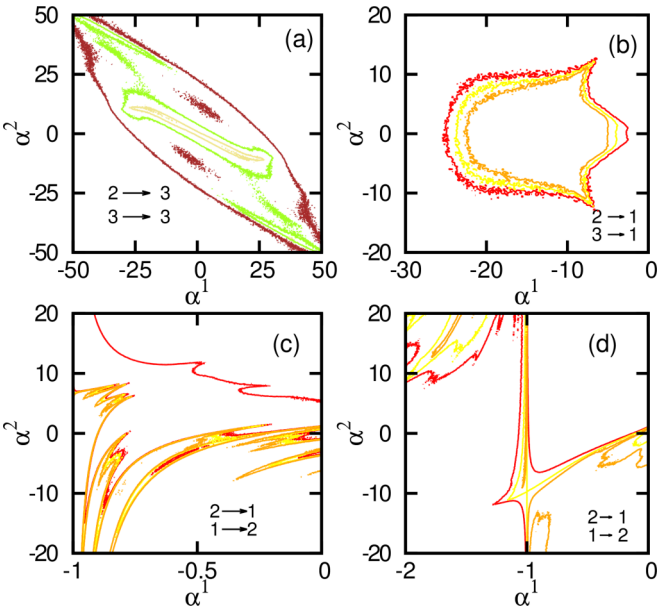

FIG. 4. (Color online) Contours of constant MSF (λ_s), obtained from Eq. (10), with coupling schemes as indicated by the pair of arrows. Figures (a) and (b) correspond to coupled Lorenz flows. In (a) the contours correspond to (green) $\lambda_s = 1.0$, (khaki) $\lambda_s = 2.0$, and (brown) $\lambda_s = 3.0$, while in (b) the contours correspond to $\lambda_s = -0.2, 0.0, 0.2$. Figure (c) is for coupled driven Duffing oscillators with the contours corresponding to $\lambda_s = -0.022, 0, 0.022, 1$, and (d) the driven van der Pol systems with the contours corresponding to $\lambda_s = -0.022, 0, 0.022, 1$. The color codes in (b)–(d) are positive (red), negative (orange), and zero (yellow) contours.

forms of the MSF were observed when the row sums δ^k of connectivity matrices $\mathbf{G}^k$ are zero. However, the basic forms of these MSFs are preserved when $\delta^k \sim 0$. This facilitates location of regions of synchronization (and/or amplitude death) in the α^1-α^2 plane. In general, synchronization or amplitude death in hypernetworks can be observed in the α^1-α^2 plane on a family of curves within the synchronization region as indicated by the MSF.

It is interesting to note that the shape of contours in the α^1-α^2 plane can be predicted from the contours of the sum of MSF's corresponding to a single network. Say the MSF for the coupling scheme $i \to j$ as a function of α, where α is the scaled eigenvalue when only one connection matrix is taken, is given by $\Lambda_s = \eta_{ij}(\alpha)$. The sum of two such Λ_s with $i = 1$ (meaning the coupling term is introduced in the equation for the first variable) and $j = 2,3$ can be Taylor expanded in powers of α^1 and α^2 about (0,0) as follows:

$$\begin{aligned}\Lambda_s(\alpha^1) + \Lambda_s(\alpha^2) &= \eta_{12}(\alpha^1) + \eta_{13}(\alpha^2) \\ &= \eta_{12}(0) + \eta_{13}(0) + \alpha^1 \partial_{\alpha^1}\eta_{12} + \alpha^2 \partial_{\alpha^2}\eta_{13} \\ &\quad + \frac{1}{2!}\left((\alpha^1)^2 \partial^2_{\alpha^1}\eta_{12} + (\alpha^2)^2 \partial^2_{\alpha^2}\eta_{13}\right). \quad (11)\end{aligned}$$

For a constant value of LHS Eq. (11) defines a curve in the α^1-α^2 plane. Now consider the master stability function of a hypernetwork $\Lambda_s(\alpha^1,\alpha^2)$. Carrying out the Taylor expansion would give

$$\begin{aligned}\Lambda_s(\alpha^1,\alpha^2) &= \eta_{23}(\alpha^1,\alpha^2) \\ &= \eta_{23}(0,0) + \alpha^1 \partial_{\alpha^1}\eta_{23} + \alpha^2 \partial_{\alpha^2}\eta_{23} \\ &\quad + \frac{1}{2!}\left((\alpha^1)^2 \partial^2_{\alpha^1}\eta_{23} + (\alpha^2)^2 \partial^2_{\alpha^2}\eta_{23}\right) \\ &\quad + \alpha^2\alpha^1 \partial_{\alpha^1}\partial_{\alpha^2}\eta_{23}, \quad (12)\end{aligned}$$

where we have dropped the index referring to the subequation in which coupling terms are present, i.e., $i = 1$ in this specific instance.

Depending on the sign of the coefficients of powers of α^1 and α^2 near the transition to a particular value in $\Lambda_s(\alpha^1,\alpha^2)$ and $\Lambda_s(\alpha^1,\alpha^2)$, topologically identical contours in the α^1-α^2 plane are formed by the two functions. However, since the function $\Lambda_s(\alpha^1,\alpha^2)$ may have terms of interaction type $(\alpha^1)^{p_1}(\alpha^2)^{p_2}$, where p_1, p_2 are integer powers, the topological form of the contours in the functions in Eq. (11) and Eq. (12) may differ. This gives necessary (but not sufficient) conditions for identical contour types observed in the hypernetwork MSF: compare Figs. 3 and 4 with Fig. 5. The sum of MSF's test, as argued above, is computationally simple to perform. To test the robustness of MSF forms under parameter mismatch, we numerically calculate λ_s from Eq. (10) for various values of ψ^1 and ψ^2. We observe that if the parameter variation is *sufficiently small* as embodied in ψ^1 or ψ^2, the shapes of MSF are robust. The perturbative condition varies depending on the choice of parameter(s) that have the mismatch, and representative cases for the Rössler and Lorenz flows are shown in Fig. 6. Note that the basic character of the MSF is robust when the row sum for the $G^{1,2}$ matrices is small.

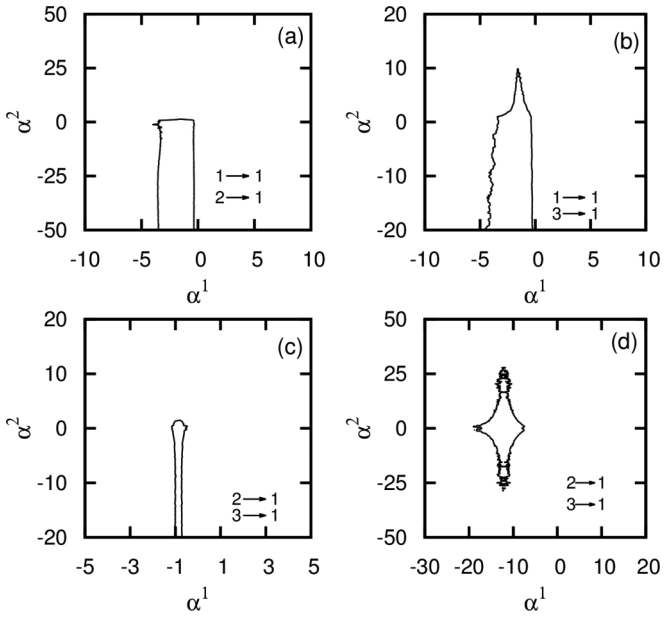

FIG. 5. Contours of the sum of the MSF for single networks in the α^1-α^2 plane for the (a),(b) Rössler, (c) Hindmarsh-Rose neuron, and (d) Lorenz flows with the coupling scheme indicated (compare with Figs. 3 and 4). Shown are contours of zero sum. Two arrows in each subfigure indicate that MSF's with these coupling schemes have been added to obtain the contour(s).

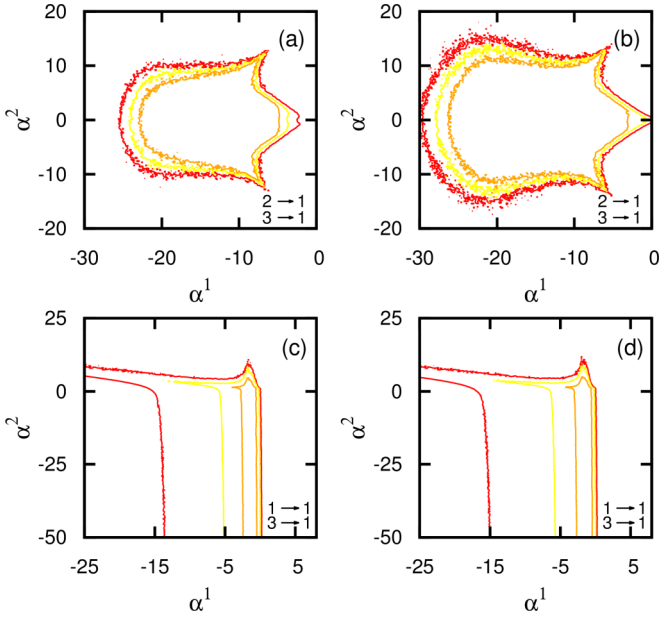

FIG. 6. (Color online) Contours of constant MSF (λ_s) positive (red), negative (orange), and zero (yellow) in the α^1-α^2 plane for coupled Lorenz flows with (a),(b) $\psi^2 = 0.1, 1.0$ and Rössler oscillators in (c),(d) with $\psi^2 = 0.05, 0.1$. Compare with Figs. 3 and 4. The coupling scheme of the hypernetwork is indicated by the pair of arrows in each subfigure. [Note that in Fig. 4(b) the value of ψ^2 is zero; hence the similarity to Fig. (a) above.]

IV. SUMMARY

In this work, we have investigated the master stability function of a hypernetwork numerically and showed that it can be classified into open and closed stable regions of synchronization. The MSF's are robust under small variation of parameters. The topology of hypernetwork MSF's can be predicted using MSF sums of the single network, as a necessary but not sufficient condition. The robustness of the basic nature of these MSF curves follows from the conjecture that convergence to synchronization states depend smoothly on parameter mismatch [28,29].

We also showed that synchronization with the conjugate diffusive coupling introduced in [2,3] can be fully understood in terms of MSF of a hypernetwork when the sum δ^k of each of the connection matrices [$\mathbf{G}^k$ in Eq. (6)] is a nonzero constant. For sufficiently small δ^k one can obtain the phenomenon of amplitude death, thus providing a basis for the observation of amplitude death in conjugate coupled systems with identical parameters to be understood in terms of possible states of a hypernetwork.

The occurrence of bounded and unbounded regions of synchronized dynamics is found here when the coupling is of diffusive type. In experimental and model situations when the coupling is linear, the present study will be useful in predicting synchronization regimes. However, there are examples of systems where the coupling is nonlinear [35], and in these cases our approach may provide the first step in a perturbative analysis. As is well known, the MSF formalism is not applicable for coupling schemes dominated by higher-order terms, and such hypernetworked systems will need to be investigated separately.

ACKNOWLEDGMENTS

S.B. is supported by the CSIR, India through a Senior Research Fellowship and R.R. by the DST through JC Bose fellowship.

APPENDIX: MODEL SYSTEMS

In this paper we have studied hypernetwork coupling in the following dynamical systems.

(i) Rössler flow [36]:

$$\begin{aligned} \dot{x}_1^i &= -a x_2^i - x_3^i, \\ \dot{x}_2^i &= a x_1^i + b x_2^i, \\ \dot{x}_3^i &= c + x_3^i (x_1^i - d), \end{aligned} \tag{A1}$$

with $a = 0.97$, $b = 0.165$, $c = 0.2$, and $d = 10$.

(ii) Lorenz flow [37]:

$$\begin{aligned} \dot{x}_1 &= \sigma(x_2 - x_1), \\ \dot{x}_2 &= x_1(r - x_3) - x_2, \\ \dot{x}_3 &= x_1 x_2 - b x_3, \end{aligned} \tag{A2}$$

with $\sigma = 10$, $r = 28$, and $b = 8/3$.

(iii) Hindmarsh-Rose neuron [38]:

$$\begin{aligned} \dot{x}_1 &= x_2 + 3x_1^2 - x_1^3 - x_3 + I, \\ \dot{x}_2 &= 1 - 5x_1^2 - x_2, \\ \dot{x}_3 &= -r x_3 + r s (x_1 + 1.6), \end{aligned} \tag{A3}$$

with $I = 3.2$, $r = 0.006$, and $s = 4$.

(iv) Driven Duffing oscillator [39]:

$$\begin{aligned} \dot{x}_1 &= x_2, \\ \dot{x}_2 &= -hx_2 - x_1^3 + q\ \sin(\eta x_3), \\ \dot{x}_3 &= 1, \end{aligned} \tag{A4}$$

with $\eta = 1$, $h = 0.1$, and $q = 5.6$.

(v) Driven van der Pol oscillator [26]:

$$\begin{aligned} \dot{x}_1 &= x_2, \\ \dot{x}_2 &= -x_1 + d\left(1 - x_1^2\right)x_2 + f\ \sin(\eta x_3), \\ \dot{x}_3 &= 1, \end{aligned} \tag{A5}$$

with $\eta = 4.065$, $d = 3$, and $f = 15$.

In all cases, the motion is chaotic for the specified set of parameters [26].

[1] P. M. Gade and C. Basu, Phys. Lett. A **217**, 21 (1996).
[2] R. Karnatak, R. Ramaswamy, and A. Prasad, Phys. Rev. E **76**, 035201 (2007).
[3] R. Karnatak, A. Prasad, and R. Ramaswamy, Chaos **19**, 033143 (2009).
[4] A. Pikovsky, M. Rosenblum, and J. Kurths, *Synchronization: A Universal Concept in Nonlinear Sciences* (Cambridge University Press, New York, 2003).
[5] E. S. Kurkina and E. D. Kuretova, Comput. Math. Model. **15**, 38 (2004).
[6] J. Imbs, Rev. Econ. Stat. **86**, 723 (2004).
[7] M. G. Rosenblum, A. S. Pikovsky, and J. Kurths, Fluct. Noise Lett. **4**, L53 (2004).
[8] B. Blasius and L. Stone, Int. J. Bifurc. Chaos **10**, 2361 (2000).
[9] L. Conradt and T. J. Roper, Proc. R. Soc. B **267**, 2213 (2000).
[10] A. Prasad, M. Dhamala, B. M. Adhikari, and R. Ramaswamy, Phys. Rev. E **81**, 027201 (2010).
[11] A. Prasad, Phys. Rev. E **72**, 056204 (2005).
[12] A. Prasad, Chaos Solitons Fractals **43**, 42 (2010).
[13] F. Sorrentino, New J. Phys. **14**, 033035 (2012).
[14] Sz. Boda, Z. Néda, B. Tyukodi, and A. Tunyagi, Eur. Phys. J. B **86**, 263 (2013).
[15] Y-C. Lai, E. M. Bolt, and Z. Liu, Chaos Solitons Fractals **15**, 219 (2003).
[16] G. Saxena, A. Prasad, and R. Ramaswamy, Phys. Rep. **521**, 205 (2012).
[17] G. Saxena, N. Punetha, A. Prasad, and R. Ramaswamy, AIP Conf. Proc. **1582**, 158 (2014).
[18] V. Pal, A. Prasad, and R. Ghosh, J. Phys. B **44**, 235403 (2011).
[19] V. Resmi, G. Ambika, and R. E. Amritkar, Phys. Rev. E **84**, 046212 (2011).
[20] L. M. Pecora and T. L. Carroll, Phys. Rev. Lett. **64**, 821 (1990).
[21] L. M. Pecora and T. L. Carroll, Phys. Rev. Lett. **80**, 2109 (1998).
[22] K. Josić, Phys. Rev. Lett. **80**, 3053 (1998).
[23] L. M. Pecora, T. L. Carrol, G. A. Johnson, and D. J. Mar, Chaos **7**, 520 (1997).
[24] J. F. Heagy, T. L. Carroll, and L. M. Pecora, Phys. Rev. E **50**, 1874 (1994).
[25] K. S. Fink, G. Johnson, T. Carroll, D. Mar, and L. Pecora, Phys. Rev. E **61**, 5080 (2000).
[26] L. Huang, Q. Chen, Y.-C. Lai, and L. M. Pecora, Phys. Rev. E **80**, 036204 (2009).
[27] Higher $(i + j)$ is assigned the higher superscript, and if the sums are equal, then the larger j has the larger superscript.
[28] J. Sun, E. M. Bollt, and T. Nishikawa, Europhys. Lett. **85**, 60011 (2009).
[29] S. Acharyya and R. E. Amritkar, Europhys. Lett. **99**, 40005 (2012).
[30] F. Sorrentino and M. Porfiri, Europhys. Lett. **93**, 50002 (2011).
[31] R. Karnatak, A. Prasad, and R. Ramaswamy, in *conference proceedings, PHYSCON 2009, Catania, Italy, 1–4 September* (2009), lib.physcon.ru/file?id=063eebebf18e.
[32] D. V. R. Reddy, A. Sen, and G. L. Johnston, Phys. Rev. Lett. **80**, 5109 (1998).
[33] R. E. Mirollo and S. H. Strogatz, J. Stat. Phys. **60**, 245 (1990).
[34] B. Ermentrout, Physica D **41**, 219 (1990).
[35] K. J. Friston, Neuroscientist **7**, 406 (2001).
[36] O. E. Rössler, Phys. Lett. A **57**, 397 (1976).
[37] E. N. Lorenz, J. Atmos. Sci. **20**, 130 (1963).
[38] J. L. Hindmarsh and R. M. Rose, Proc. R. Soc. B **221**, 87 (1984).
[39] J. Guckenheimer and P. Holmes, *Nonlinear Oscillations, Dynamical Systems, and Bifurcations of Vector Fields* (Springer-Verlag, Berlin, 1983).